

A CFD ANALYSIS OF ROOM ASPECT RATIO ON THE EFFECT OF BUOYANCY AND ROOM AIR FLOW

by

Brajesh TRIPATHI, Sandipan Ghosh MOULIC, and Late R. C. ARORA

Original scientific paper

UDC: 697.12/.13

BIBLID: 0354-9836, 11 (2007), 4, 79-94

Comfort conditions in air-conditioned rooms require that temperature in the occupied zone should not vary by more than 1 °C and velocity, everywhere in the room, should be less than 0.15 m/s so that occupants do not feel draft. Recent developments in providing effective insulation and making leak tight buildings are considerably reduced the cooling load requirements and the supply airflow rates. Obtaining uniform temperature distribution with reduced air volume flow rates requires careful design of air distribution system. This study aims to find velocity and temperature distribution in the room towards this end.

Key words: *aspect ratio, room airflow, buoyancy, comfort*

Introduction

A dry-bulb temperature of 25 °C, 50% relative humidity, 0.1-0.25 m/s air velocity and appropriate air purity are considered as comfortable summer conditions, and the buildings are designed accordingly. From a computational perspective, airflows in the rooms are very complex. The flow is fully turbulent in the supply air ducts, HVAC outlets/inlets and downstream of the edges of the obstacles. Elsewhere, the flow is more likely to be laminar or weakly turbulent and unsteady with a wide range of small to large-scale flow structures where molecular transport is important. In the context of cooling (or heating in cold climates), these flows are buoyant and in some cases, buoyancy drives the mean flow motion. The presence of walls creates so called near wall regions, where the turbulent transport is significantly influenced by a solid surface.

In practical applications, the obstructions within the room create geometrical complexity. In reality, most room airflows are inherently three-dimensional and unsteady. Shear layers on the periphery of supply air jet and recirculation within the room adds to the complexity of the flow. Due to these characteristics, airflows in room present a great challenge for the available numerical codes and models. Nowadays, very effective insulation materials are being used in air-conditioned buildings, which have considerably reduced the cooling/heating loads and thereby the air supply rates have also considerably reduced. Hence, laminar and low Reynolds number turbulent flows modelling are gaining increasing importance.

Literature review

Terai [1] made the first attempt for the numerical calculation of indoor airflow for the case of two-dimensional buoyant flow. Tsuchiya [2], Nomura and Kaizuka [3], and Yamazaki *et al.* [4] have made important contributions towards understanding of two-dimensional laminar room airflows. Many authors have reported a closely related topic of natural convection in partitioned enclosures and it has been reviewed in a recent paper by Hsu *et al.* [5]. Lee *et al.* [6] have applied finite element method to study the characteristics of forced and mixed convection in an air-cooled room for both laminar and turbulent regimes. Edward *et al.* [7] have experimentally investigated the effect of air movement on different human subjects within a room. Sherman [8] and Srebric *et al.* [9] have studied airflow and air quality for residential buildings. Costa *et al.* [10] have investigated the turbulent airflow with two jet heating system for different room aspect ratios. Sinha [11] has investigated the effect of inclined jet on room air cooling.

Gobeau and Saunders [12] have investigated the effect of inlet conditions and geometry on a turbulence model. Yi and Qingyan [13] have investigated buoyancy-driven single-sided natural ventilation with large openings. Catalin *et al.* [14] have described a numerical model to assess the thermal comfort taking into account the indoor air moisture and its transport by the airflow within an enclosure. Eftekhari and Marjanovic [15] have developed a fuzzy controller for naturally ventilated buildings. Andersen [16] has given a reliable tool for analyzing and designing natural ventilation systems where thermal buoyancy is the dominating driving force. Bin *et al.* [17] have proposed a simplified system based on a new air supply opening model and a numerical method of solving the discrete algebraic equations to accelerate and simplify the convergence procedure of predicting air distribution in ventilated rooms.

Problem formulation

In this investigation two-dimensional, steady, incompressible, laminar flow under Boussinesq's approximation has been considered. The physical properties are assumed to be constant. The velocity and temperature distributions in a room have been found by solving Navier Stokes equations and energy equation numerically by SIMPLE and SIMPLEC algorithms.

Non-dimensionalization

The inlet velocity U_{inlet} and inlet opening W_1 are taken as characteristic velocity and length, respectively. The difference between wall temperature T_w and inlet temperature T_{inlet} is used for non-dimensionalization of temperature. The non-dimensionalization scheme is as follows:

$$\begin{array}{lll}
 U & \frac{u}{U_{\text{inlet}}} & V & \frac{v}{U_{\text{inlet}}} & X & \frac{x}{W_1} \\
 Y & \frac{y}{W_1} & P & \frac{p}{\nu \rho U_{\text{inlet}}^2} & \theta & = \frac{T - T_w}{T_{\text{inlet}} - T_w} \\
 \text{Gr} & \frac{g \beta \Delta T W_1^3}{\nu^2} & \text{Re} & \frac{U_{\text{inlet}} W_1}{\nu} & \text{Pr} & = \frac{C_p \mu}{K}
 \end{array}$$

where Pr is the Prandtl number, Re is the Reynolds number, and Gr is the Grashof number. Non-dimensional form of conservation equations are:

Conservation of mass (continuity equation)

$$\frac{\partial U}{\partial X} + \frac{\partial V}{\partial Y} = 0 \quad (1)$$

Conservation of X-momentum

$$\frac{\partial(UU)}{\partial X} + \frac{\partial(VU)}{\partial Y} - \frac{\partial P}{\partial X} = \frac{1}{\text{Re}} \left(\frac{\partial^2 U}{\partial X^2} + \frac{\partial^2 U}{\partial Y^2} \right) \quad (2)$$

Conservation of Y-momentum

$$\frac{\partial(UV)}{\partial X} + \frac{\partial(VV)}{\partial Y} - \frac{\partial P}{\partial Y} = \frac{1}{\text{Re}} \left(\frac{\partial^2 V}{\partial X^2} + \frac{\partial^2 V}{\partial Y^2} \right) + \frac{\text{Gr}}{\text{Re}^2} \theta \quad (3)$$

Energy conservation equation

$$\frac{\partial(U\theta)}{\partial X} + \frac{\partial(V\theta)}{\partial Y} - \frac{1}{\text{Re Pr}} \left(\frac{\partial^2 \theta}{\partial X^2} + \frac{\partial^2 \theta}{\partial Y^2} \right) = 0 \quad (4)$$

Geometry and boundary conditions

A rectangular room 6 m long and 3 m high has been considered. For simplicity, the aerodynamic blockage due to various items in the room has been neglected. The air movement in the room has been analysed for various aspect ratios at different values of Grashof number. Three different aspect ratios have been considered as shown in figs.

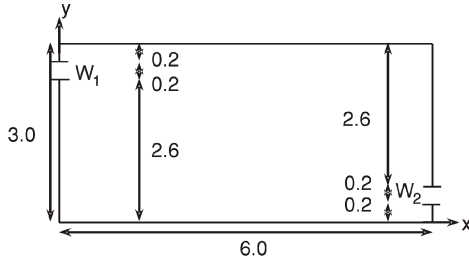


Figure 1. Room geometry (A)

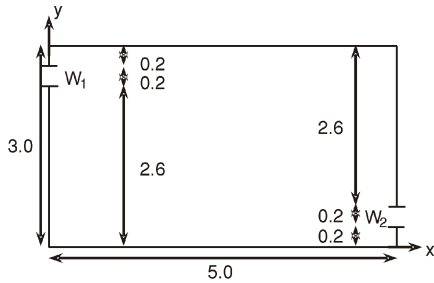


Figure 2. Room geometry (B)

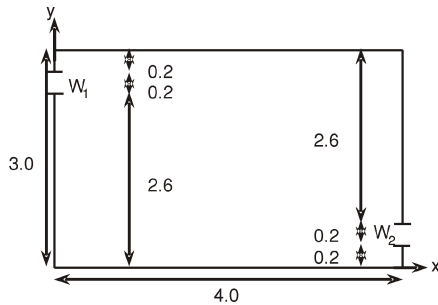


Figure 3. Room geometry (C)

1-3. No-slip and impermeability boundary conditions have been used on all walls except at inlets and outlets. The boundary conditions are:

- at the left, right, top, and bottom walls

$$U = 0, \quad V = 0, \quad \theta = 1$$

- at the inlet

$$U = 1, \quad V = 0, \quad \theta = 0$$

- at the outlet

$$\frac{\partial \phi}{\partial n} = 0, \quad \phi = U, V, \theta$$

Neumann conditions have been set for the flow variables as above. Where n is the direction normal to the outflow boundary. In addition, mass conservation has also been satisfied at the outlet.

Numerical solution procedure

The computational domain shown in fig. 1 has been divided into non-overlapping control volumes. Fine grids have been chosen near the walls, inlet, and outlet. These have been slowly expanded to coarse grids in the interior of room. Grid points are located at the center of the control volumes where the scalar variables such as pressure, density and temperature are defined. Grid points are also located on the boundaries for convenience of specifying the boundary conditions. In this

case, the room has been divided into 80×92 grids in x-y direction.

The discretized equations are obtained by integrating Navier-Stokes and energy equations over the control volumes. Assuming familiarity with the SIMPLE algorithm due to Patankar [18] and SIMPLEC algorithm due to Van Doormaal *et al.* [19], the details are omitted. The numerical solutions were compared with benchmark experimental results reported by Nielsen [20]. The inlet and outlet were slots extending throughout the width of the room. Inlet and outlet were located on top of the left wall and bottom of the right wall, respectively.

Figure 4 shows a comparison of the horizontal velocity (U) at the vertical cross-section of the room. These experimental results are at the central plane where the two-dimensional numerical predictions can be compared with the measured data of three-dimensional case. The agreement is observed to be good in the region of laminar or weakly turbulent flow. It is not satisfactory in the region of mainstream near the ceiling, where the turbulent flow contains variations on a much wider range of length and time scales than the laminar flow. Therefore, it can be concluded that the solutions of laminar flows can be used for quick, economic and approximate predictions for room air distribution.

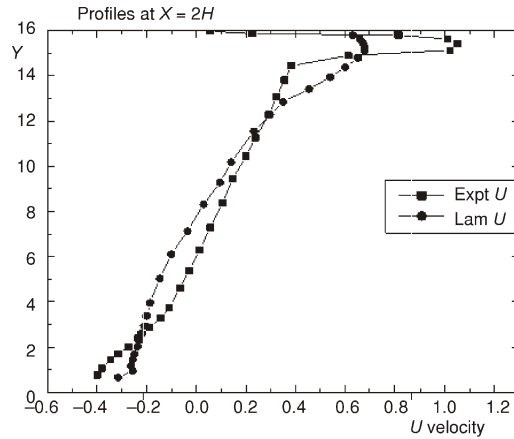


Figure 4. Velocity (U) profile at $X/H = 2$

Results and discussion

The computed distributions of streamlines and isotherms in room are illustrated in figs. 5 to 22 for the case of cooling (inlet near the ceiling on left wall and outlet near to floor on right wall) at different aspect ratios and for Reynolds number, $Re = 2000$ and different values of Gr/Re^2 ranging from 0.01 to 0.2. It has been observed that the cold primary air enters in the room near the ceiling and attaches with the ceiling due to Coanda effect. It moves along the ceiling for some distance and then either moves towards the opposite wall and comes

down along the wall to go out or stoops downwards, attaches with the floor and then goes out depending upon Gr . Figure 5 shows that at $Re = 2000$ and $Gr/Re^2 = 0.01$, it stoops downwards. As buoyancy increases further, the point of attachment on floor moves towards the inlet as seen in fig. 11. Two circulation zones

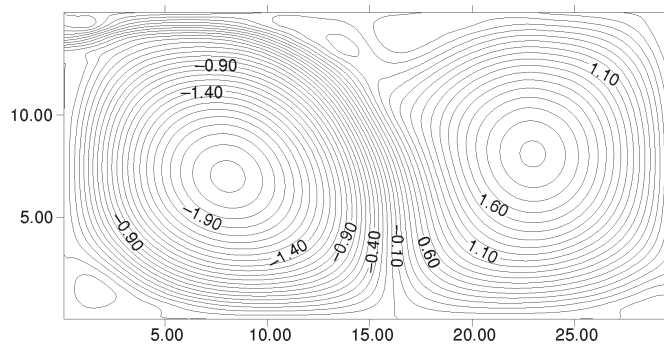


Figure 5. Streamlines for $Re = 2000$, $Gr/Re^2 = 0.01$ for case (A)

are observed due to entrainment. The extent of circulation increases with increases in Grashof number.

Figures 6 and 12 show that temperature variation is confined to thermal boundary layers on the walls. The temperature becomes more uniform in the recirculating region. As the aspect ratio decreases to 5/3 in case (B), the point of attachment on the floor moves towards the right wall as shown in fig. 7. The flow touches the right wall as the aspect ratio further decreases to 4/3 in the case (C) as shown in fig. 9. A small anticlockwise

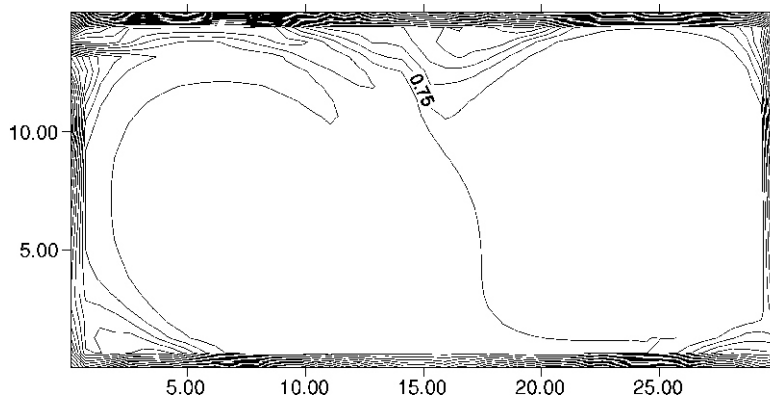


Figure 6. Isotherms for $Re = 2000$, $Gr/Re^2 = 0.01$ for case (A)

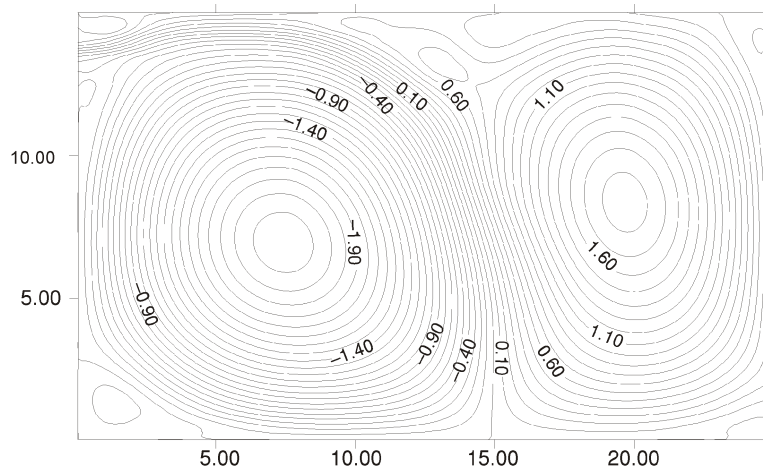


Figure 7. Streamlines for $Re = 2000$, $Gr/Re^2 = 0.01$ for case (B)

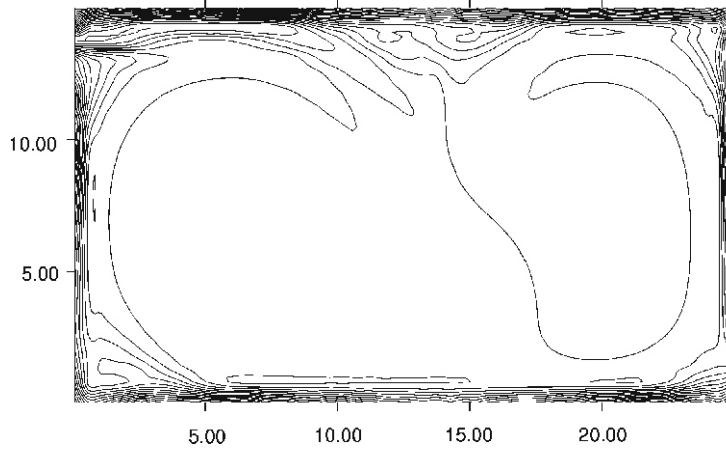


Figure 8. Isotherms for $Re = 2000$, $Gr/Re^2 = 0.01$ for case (B)

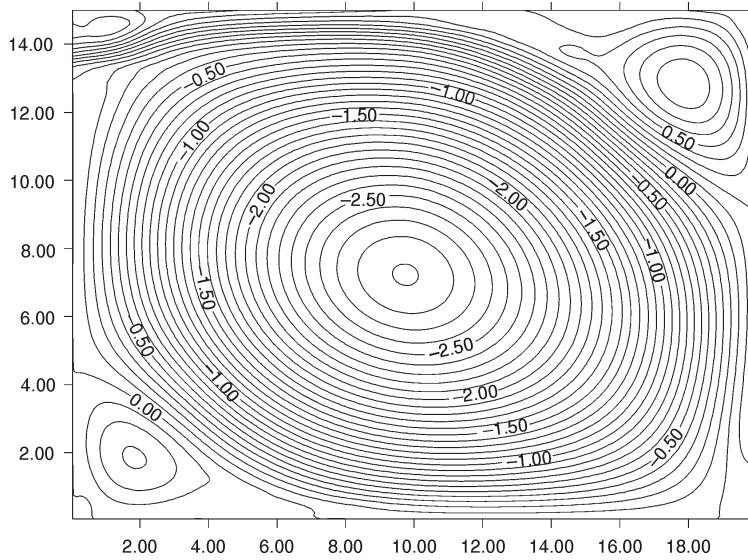


Figure 9. Streamlines for $Re = 2000$, $Gr/Re^2 = 0.01$ for case (C)

recirculatory cell is observed in the top right corner due to warm air rising along the right wall. The point of attachment moves towards the inlet with increase in buoyancy.

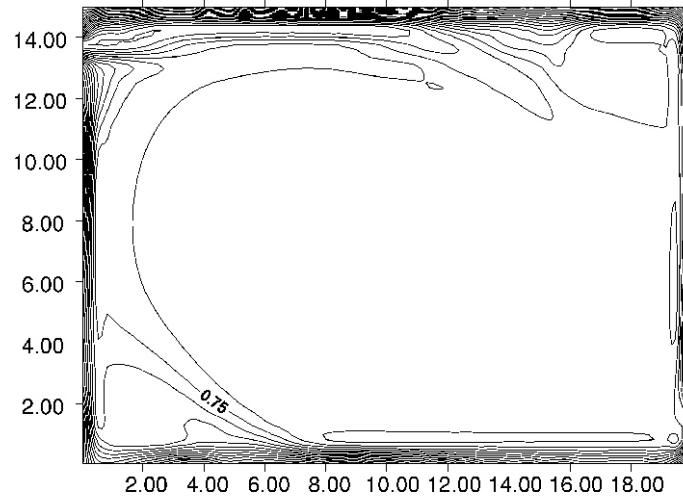


Figure 10. Isotherms for $Re = 2000$, $Gr/Re^2 = 0.01$ for case (C)

The flow pattern has been found to be similar in all the cases of different aspect ratios. Both the left and right walls are at higher temperature than inlet. Therefore, the secondary flow rises up along both the walls in the natural convection boundary layer due

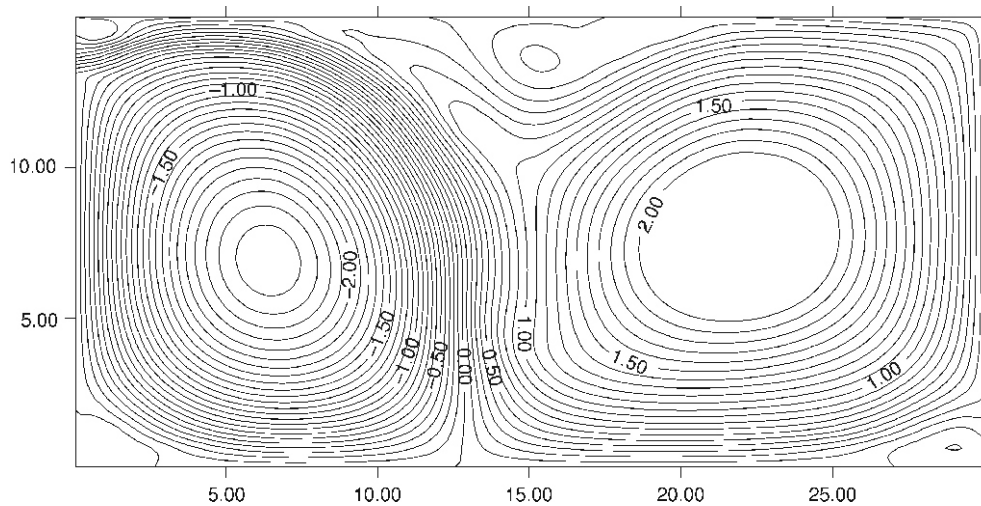


Figure 11. Streamlines for $Re = 2000$, $Gr/Re^2 = 0.1$ for case (A)

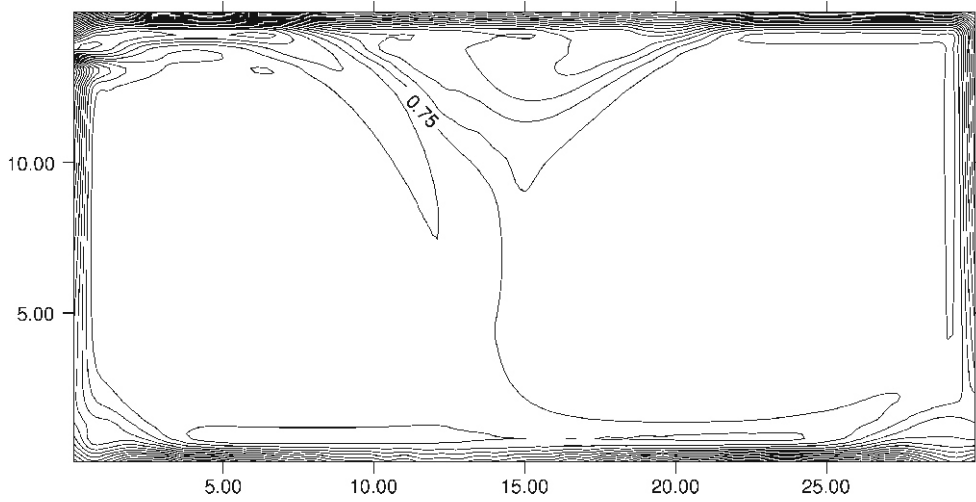


Figure 12. Isotherms for $Re = 2000$, $Gr/Re^2 = 0.1$ for case (A)

to buoyancy. The temperature is observed to be uniform in both the recirculation zones. Figures 11, 13, and 15 shows the streamlines for $Re = 2000$ and $Gr/Re^2 = 0.1$ for aspect ratios of 2.0, 5/3, and 4/3, respectively. It is observed that as Grashof number increases the point of attachment on the floor moves towards the left wall since the intensity of

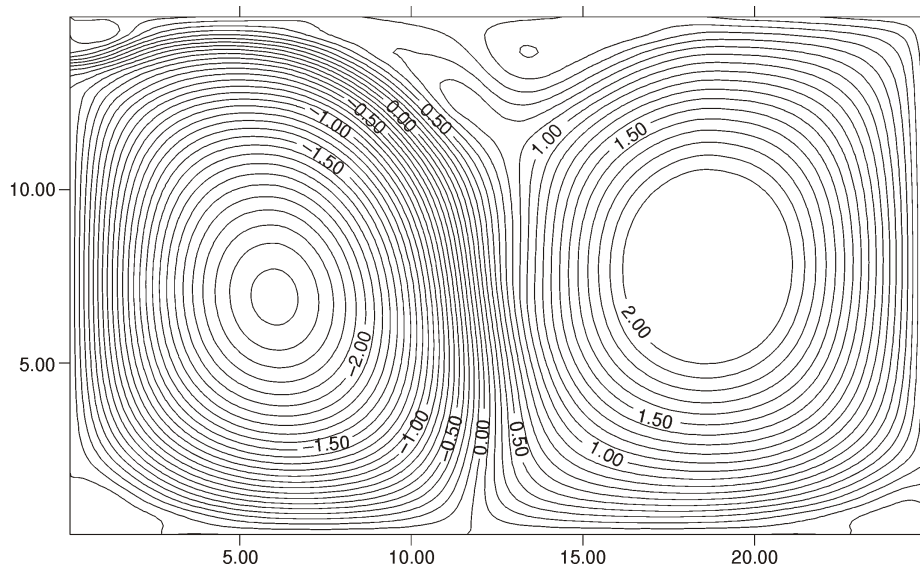


Figure 13. Streamlines for $Re = 2000$, $Gr/Re^2 = 0.1$ for case (B)

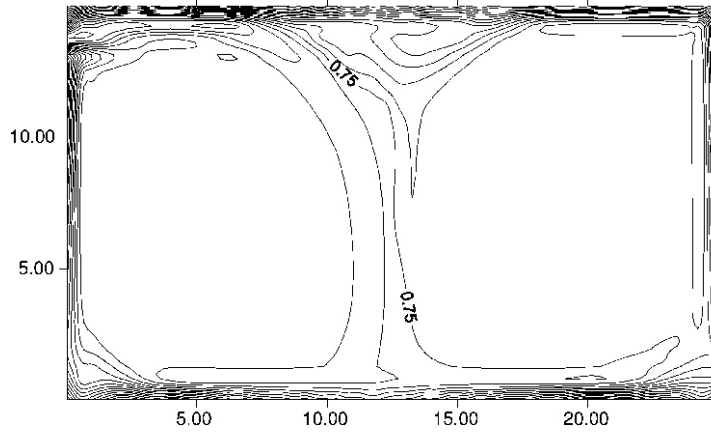


Figure 14. Isotherms for $Re = 2000$, $Gr/Re^2 = 0.1$ for case (B)

recirculation cell near left wall increases. The flow at aspect ratio of 4/3 also attaches with the floor as seen in fig. 15. Isotherms reveal that temperature variation is confined to wall boundary layer. There is some variation in temperature near stagnation zones as shown in figs. 12, 14, and 16.

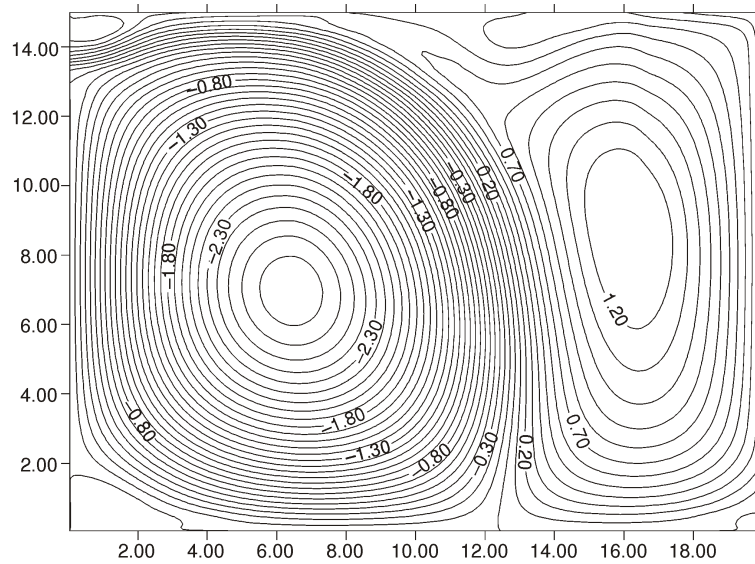


Figure 15. Streamlines for $Re = 2000$, $Gr/Re^2 = 0.1$ for case (C)

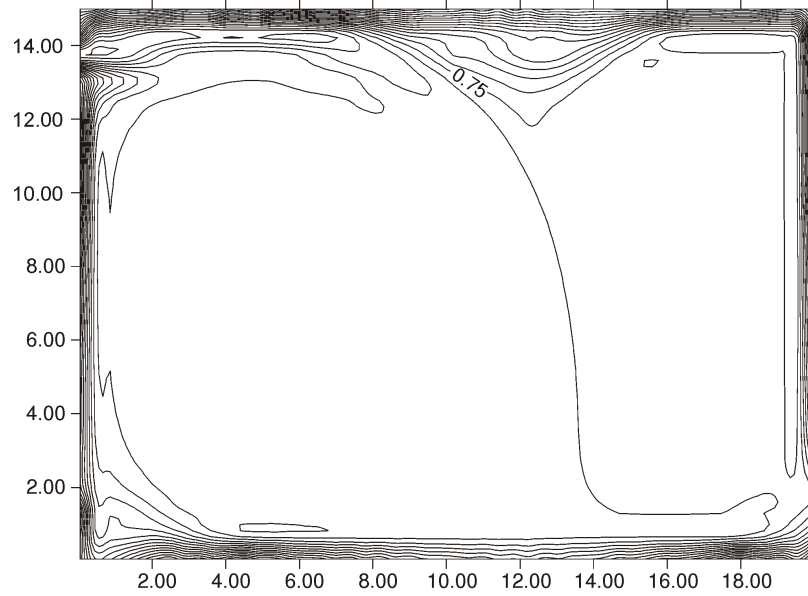


Figure 16. Isotherms for $Re = 2000$, $Gr/Re^2 = 0.1$ for case (C)

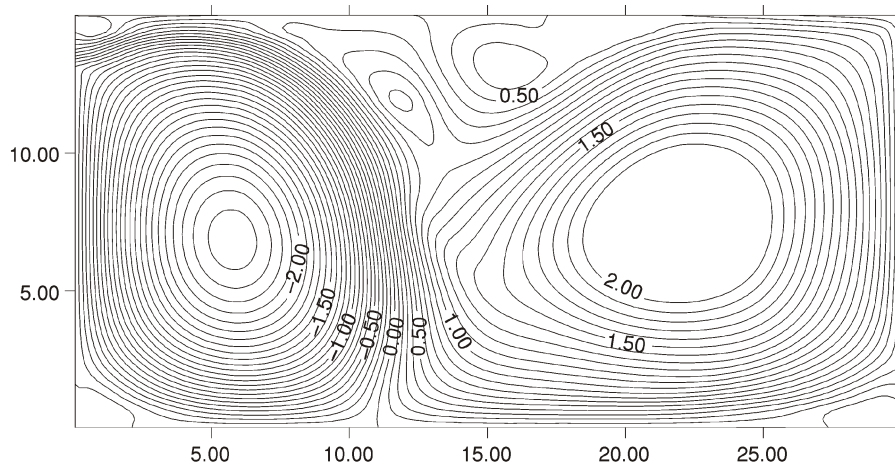


Figure 17. Streamlines for $Re = 2000$, $Gr/Re^2 = 0.2$ for case (A)

Figures 17-22 shows similar results for $Gr/Re^2 = 0.2$. The intensity of clockwise recirculation continues to increase and its size continuous to decrease with increase in Gr/Re^2 for all aspect ratios. The effect of buoyancy seems to be more pronounced at

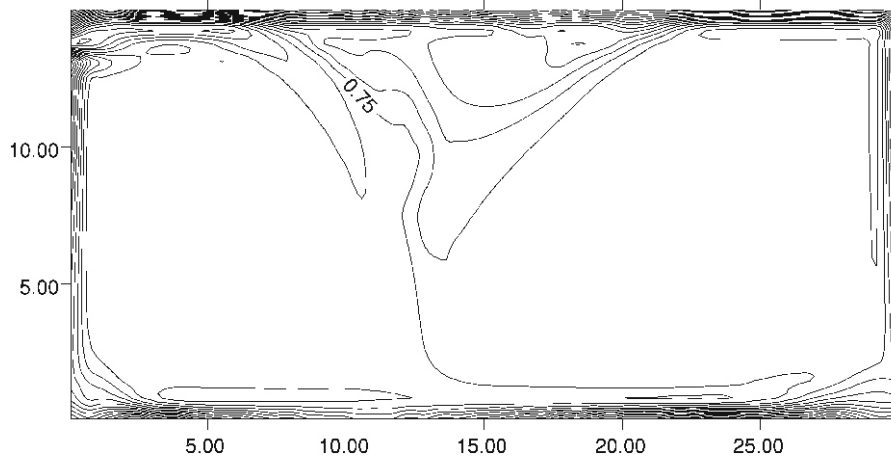


Figure 18. Isotherms for $Re = 2000$, $Gr/Re^2 = 0.2$ for case (A)

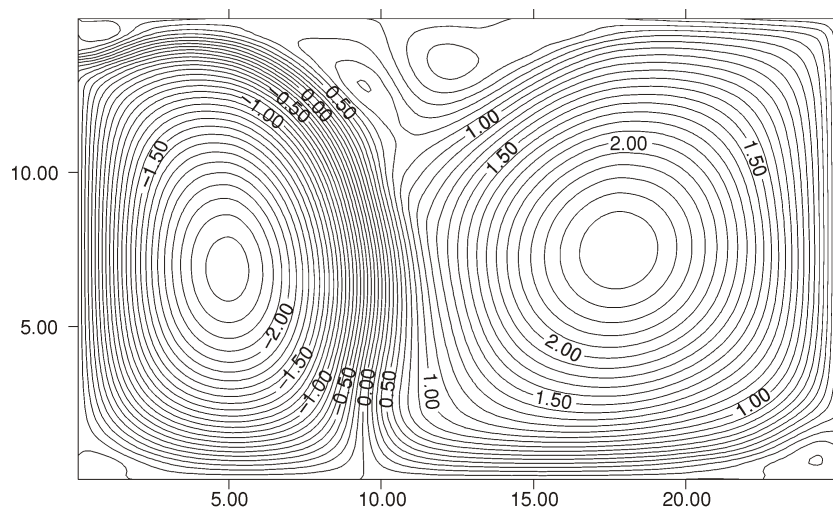


Figure 19. Streamlines for $Re = 2000$, $Gr/Re^2 = 0.2$ for case (B)

smaller aspect ratios. For aspect ratio of $4/3$ at $Gr/Re^2 = 0.2$ the clockwise recirculation cell is smallest in size and has largest intensity compared to that at large aspect ratios. The recirculation cell due to Coanda effect tends to disappear for aspect ratio of $4/3$ as Gr/Re^2 increases. At $Gr/Re^2 = 0.2$, two more counter rotating cells appear near the ceiling in the middle of the room. These are more pronounced for larger aspect ratio. Recirculatory cells make appearance at both the corners on the floor also.

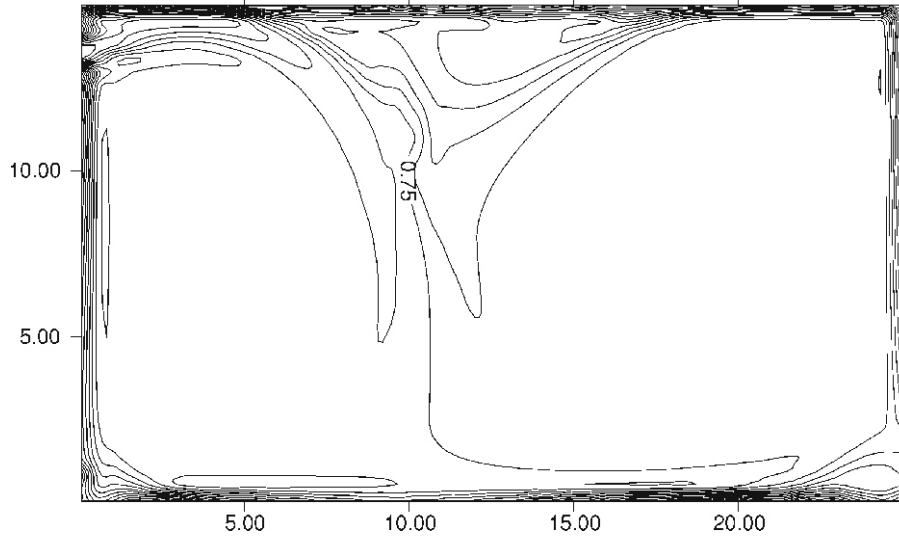


Figure 20. Isotherms for $Re = 2000$, $Gr/Re^2 = 0.2$ for case (B)

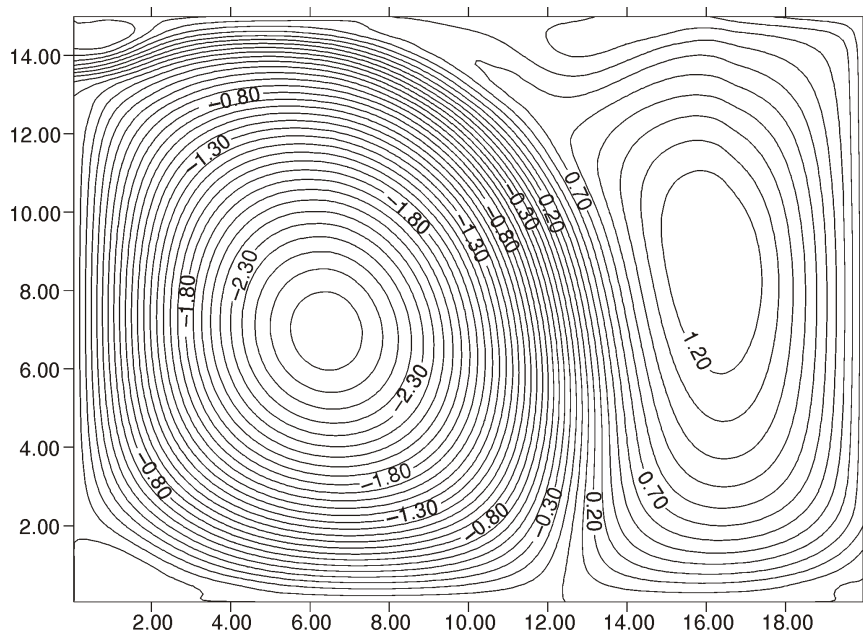


Figure 21. Streamlines for $Re = 2000$, $Gr/Re^2 = 0.2$ for case (C)

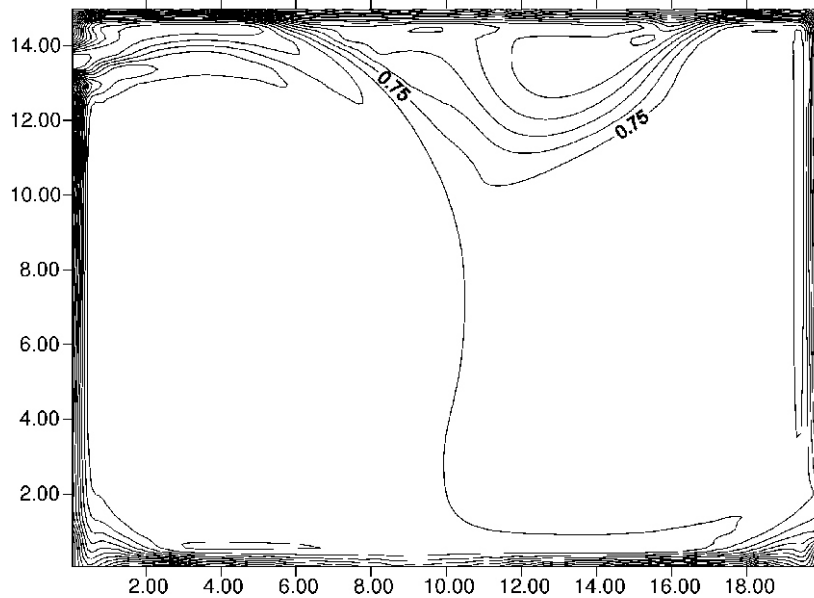


Figure 22. Isotherms for $Re = 2000$, $Gr/Re^2 = 0.2$ for case (C)

Conclusions

The cold fluid has a tendency to flow downwards due to buoyancy while the hot fluid rises up. Coanda effect, effect of buoyancy and wall boundary layers has been observed in this investigation. The Coanda effect is observed in all the cases of laminar flow except at large Gr/Re^2 and small aspect ratio. If cold fluid enters in the room near the ceiling, the flow attaches with the ceiling for different values of Gr . For small values of Gr , it continuous along the ceiling comes down along the right wall and goes out from outlet.

With increases in Gr/Re^2 , that is, as the buoyancy increases, it stoops down towards the floor in the middle of the room, flows along the floor and goes out. For small aspect ratio of room, it stoops down towards the floor at larger values of Gr/Re^2 . Once it attaches with the floor, the room airflow consists of a clockwise circulating cell near left wall and an anticlockwise circulating cell near right wall. The intensity of recirculation of both the cells increases with increase in Gr/Re^2 . The rate of increase is more pronounced at smaller aspect ratios.

Temperature variation is confined to a narrow region near the ceiling and in boundary layers on the walls. The temperature is more or less uniform throughout the room except for the region near the stagnation point. The uniformity of temperature increases as the value of Gr/Re^2 increases. The effects of Re , Gr/Re^2 , and aspect ratio has been investigated.

Nomenclature

Gr	– Grashof number ($= g\beta\Delta TW_1^3/\nu^2$), [-]
g	– acceleration due to gravity, [ms^{-2}]
K	– thermal conductivity, [$\text{Wm}^{-1}\text{K}^{-1}$]
Pr	– Prandtl number ($= C_p\mu K^{-1}$), [-]
p	– pressure of fluid, [Nm^{-2}]
Re	– Reynolds number ($= U_{\text{inlet}}W_1/\nu$), [-]
T	– temperature of fluid, [K]
T_{inlet}	– inlet temperature of fluid, [K]
T_w	– wall temperature, [K]
ΔT	– difference between inlet and wall temperature, [K]
u	– x component of velocity, [ms^{-1}]
U_{inlet}	– inlet velocity in x-direction, [ms^{-1}]
v	– y component of velocity, [ms^{-1}]
W_1, W_2	– inlet and outlet widths, respectively, [m]
x, y	– rectangular Cartesian co-ordinates, [-]

Greek symbols

β	– coefficient of thermal expansion, [K^{-1}]
μ	– absolute viscosity of fluid, [$\text{kgm}^{-1}\text{s}^{-1}$]
ν	– kinematic viscosity, [m^2s^{-1}]
ρ	– reference density of the fluid, [kgm^{-3}]

References

- [1] Terai, T., Indoor Thermal Convection, *Transaction of Architectural Institution of Japan* (in Japanese), 1 (1959), 4, pp. 63-78
- [2] Tsuchiya, T., Application of Meteorological Numerical Calculation Method to Indoor Airflows, *Transaction of Architectural Institution of Japan* (in Japanese), 4 (1973), 2, pp. 172-187
- [3] Nomura, T., Kaizuka, M., Numerical Calculation Method of Air Distribution, *Transaction of Architectural Institution of Japan* (in Japanese), 4 (1973), 3, pp. 31-39
- [4] Yamazaki, H., Urano, Y., Nashida, M., Watanabe, T., Comparison of Numerical Calculation and Visualization Experiments of Two-Dimensional Flows, *Transaction of Architectural Institution of Japan* (in Japanese), 6 (1976), 3, pp. 240-248
- [5] Hsu, T. H., Hsu, P. T., How, S. P., Mixed Convection in a Partially Divided Rectangular Enclosure, *Numerical Heat Transfer, Part A*, 31 (1997), 6, pp. 655-683
- [6] Lee, S. C., Cheng, C. Y., Chen, C. K., Finite Element Solutions of Laminar and Turbulent Flows with Forced and Mixed Convection in an Air-Cooled Room, *Numerical Heat Transfer, Part A*, 31 (1997), 5, pp. 529-550
- [7] Edward, A., Tengfang, X., Katsuhiko, M., Zhang, H., Fountain, M., Bauman, F., A Study of Occupant Cooling by Personally Controlled Air Movement”, *Energy and Building*, 27 (1998), 1, pp. 45-59
- [8] Sherman, M., Indoor Air Quality for Residential Buildings, *ASHRAE Journal*, 27 (1999), 5, pp. 26-30

- [9] Srebric, J., Chen, Q., Glickman, L. R., A Coupled Airflow and Energy Simulation Program for Indoor Thermal Environmental Studied, *ASHRAE Transactions, Part I*, 106 (2000), 1, pp. 465-476
- [10] Costa, J. J., Oliveira, L. A., Blay, D., Turbulent Airflow in a Room with a Two-Jet Heating-Ventilation System – A Numerical Study, *Energy and Building*, 32 (2000), 3, pp.327-343
- [11] Sinha, S. L., Behavior of Inclined Jet on Room Cooling, *Building and Environment*, 36 (2001), 5, pp. 569-578
- [12] Gobeau, N., Saunders, C. J., Computational Fluid Dynamics (CFD) Validation of the Prediction of Pesticide Dispersion in a Naturally-Ventilated Building, *Proceedings*, 8th International Conference Air Distribution in Rooms, Roomvent 2002, Copenhagen, pp. 697-700
- [13] Yi, J., Qingyan, C., Buoyancy-Driven Single-Sided Natural Ventilation in Buildings with Large Openings, *International Journal of Heat and Mass Transfer*, 46 (2003), 6, pp. 973-988
- [14] Catalin, T., Raluca, H., Gilles, R., Monika, W., Numerical Prediction of Indoor Air Humidity and Its Effect on Indoor Environment, *Building and Environment*, 38 (2003), 5, pp. 655-664
- [15] Eftekhari, M. M., Marjanovic, L. D., Application of Fuzzy Control in Naturally Ventilated Buildings for Summer Conditions, *Energy and Buildings*, 35 (2003), 7, pp. 645-655
- [16] Andersen, Karl T., Theory for Natural Ventilation by Thermal Buoyancy in One Zone with Uniform Temperature, *Building and Environment*, 38 (2003), 11, pp. 1281-1289
- [17] Bin, Z., Xianting, L., Qisen, Y., A Simplified System for Indoor Airflow Simulation, *Building and Environment*, 38 (2003), 4, pp. 543-552
- [18] Patankar, S. V., Numerical Heat Transfer and Fluid Flow, Hemisphere Publ. Comp., Washington DC, USA, 1980
- [19] Doormaal, Van J. P., Raithby, G. D., Enhancement of the SIMPLE Method for Predicting Incompressible Fluid Flow, *Numerical Heat Transfer*, 17 (1984), 1, pp. 147-163
- [20] Nielsen, P. V., Specification of a Two-Dimensional Test Case, Energy Conservation in Buildings and Community Systems, Annex 20: Air Flow Pattern within Buildings, International Energy Agency, 1990

Authors' address:

B. Tripathi, S. G. Moulic, L. R. C. Arora
 Department of Mechanical Engineering,
 Indian Institute of Technology, Kharagpur,
 West Bengal, 721302, India

Corresponding author B. Tripathi
 E-mail: brajesh@mech.iitkgp.ernet.in

Paper submitted: October 24, 2006
 Paper revised: March 5, 2007
 Paper accepted: October 19, 2007